ChemComm

Dynamic Nuclear Polarization of Biocompatible ^{13}C-Enriched Carbonates for *In vivo* pH Imaging

D. E. Korenchan,[a,b] R. R. Flavell,[b] C. Baligand,[b] R. Sriram,[b] K. Neumann,[b] S. Sukumar,[b] H. VanBrocklin,[b] D. B. Vigneron,[a,b] D. M. Wilson[b],* and J. Kurhanewicz[a,b],*

A hyperpolarization technique using carbonate precursors of biocompatible molecules was found to yield high concentrations of hyperpolarized ^{13}C bicarbonate in solution. This approach enabled large signal gains for low-toxicity hyperpolarized [13]C pH imaging in a phantom and *in vivo* in a murine model of prostate cancer.

Extracellular acidification has been demonstrated in a variety of cancers[1] and plays an important role in both disease progression[1-6] and in treatment efficacy.[1,7] Although interstitial pH (pH_e) has traditionally been measured in both animals and humans using microelectrodes,[1] recent efforts have focused on developing non-invasive and accurate pH imaging techniques that might be used in cancer patients. In vivo, pH_e has been studied using positron emission tomography (PET),[8-11] [1]H and ^{31}P MR spectroscopic imaging,[12-14] relaxivity-based pH_e mapping,[15,16] and chemical exchange saturation transfer (CEST).[17,18] Hyperpolarized (HP) ^{13}C magnetic resonance spectroscopic imaging (MRSI), enabled by MR signal enhancement on the order of 10^4-10^5 via dynamic nuclear polarization (DNP),[19] has enabled the study of several metabolic and transport processes relevant to cancer[20,21] and has been applied to human prostate cancer imaging in phase I clinical trials.[22] Several HP molecules have been evaluated for their ability to measure pH_e,[23,24] notably ^{13}C-bicarbonate, which uses the measured bicarbonate to CO_2 ratio and a modified Henderson-Hasselbalch equation[25] to calculate the pH_e in individual volume elements (voxels). HP ^{13}C-bicarbonate is currently limited either by the maximum ^{13}C-bicarbonate concentration and degree of polarization,[26] which in turn limits

HP signal and image resolution, or by introducing toxic species, such as Cs^+ ions[25,27] or peroxide radicals,[28] which may prohibit eventual clinical use.

In our work with HP sodium ^{13}C-bicarbonate ($NaHCO_3$) in glycerol, formulated as previously reported,[26] we frequently observed via ^{13}C spectroscopy at 11.7 T two unknown spectral peaks just upfield of the ^{13}C HCO_3^- resonance (Figure S1), which may be glycerol-bicarbonate adducts formed during heating of the [13]C $NaHCO_3$/glycerol sample. We also noted that these two peaks are absent from spectra acquired at thermal equilibrium, suggesting these transient species quickly decompose in aqueous media back to bicarbonate and glycerol. This suggested a new approach to hyperpolarizing ^{13}C-bicarbonate: polarization of a carbonated precursor followed by rapid base-catalyzed hydrolysis in the post-dissolution step.
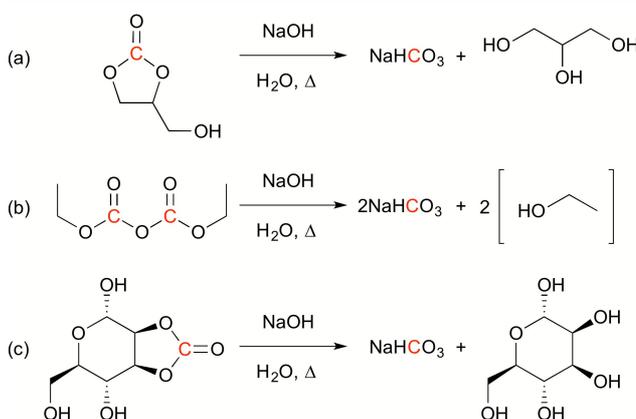

Figure 1. Hydrolysis reaction schemes for the three molecules evaluated in this study: (a) 1,2-glycerol carbonate; (b) diethyl pyrocarbonate; (c) 2,3-O-carbonyl-α-D-mannopyranose. These compounds rapidly decompose to $NaHCO_3$ and glycerol, ethanol, and D-mannose, respectively, in the presence of sodium hydroxide and heat after dissolution. Nuclei of interest for hyperpolarized ^{13}C NMR are highlighted in red.

a. UC Berkeley-UCSF Graduate Program in Bioengineering, University of California, Berkeley and University of California, San Francisco, California, USA.
b. Department of Radiology and Biomedical Imaging, University of California, San Francisco, California, USA.
* To whom correspondence should be addressed: john.kurhanewicz@ucsf.edu; david.m.wilson@ucsf.edu

COMMUNICATION
<div align="right">Journal Name</div>

Table 1. Evaluation of carbonated analogs for generating HP bicarbonate

| Molecule[a]	Concentration, M[b]	% HCO_3^- + CO_2 [c]
GLC	11.9	92.7 ± 1.4
DEPC	6.0	67.9 ± 6.7
MC	4.3	96.4 ± 1.8

[a]GLC: 1,2-glycerol carbonate; DEPC: diethyl pyrocarbonate; MC: 2,3-O-carbonyl-α-D-mannopyranose

[b]DNP substrate concentration in optimized formulation. Note that each mole of DEPC produces 2 moles of HCO_3^-.

[c]Determined as HCO_3^- + CO_2 signal over total HP signal.

We began by investigating carbonated small molecules that could be hyperpolarized and hydrolyzed to form HP ^{13}C $NaHCO_3$. Although many such molecules exist, we constrained our list to carbonates of biocompatible molecules. We also narrowed our focus to DNP substrates that are liquids at room temperature or highly water-soluble, since these compounds are more amenable to high-concentration preparation.[20,21] We thus chose three molecules to evaluate, which were carbonated analogs of glycerol, ethanol, and mannose (Figure 1). Each non-^{13}C-enriched compound was formulated for DNP at the maximum concentration possible that could both dissolve 15 mM of trityl radical and form a glass at cryogenic temperatures. An equimolar amount of each formulation was then polarized and dissolved with 2 equivalents of NaOH and 5 s of heating, followed by neutralization with HCl (n = 3 each). HP ^{13}C spectra were immediately obtained at 11.7 T to compare the extent of hydrolysis under these reaction conditions. Table 1 summarizes these results. We chose to proceed forward with 1,2-glycerol carbonate (GLC) because it offered the best combination of high formulation concentration and rapid hydrolysis.

We then developed a synthesis of [1-^{13}C] 1,2-glycerol carbonate (^{13}C-GLC) to evaluate its utility for HP pH imaging (Scheme 1). The synthesis was modified from that reported by Parameswaram et al[29] and is described in full in the Electronic Supplementary Information. Briefly, ^{13}C-dimethyl carbonate and glycerol were heated with potassium carbonate and magnesium oxide, and the resulting mixture was gravity-filtered and distilled to yield a colorless, viscous oil. The overall reaction yield was 78%.
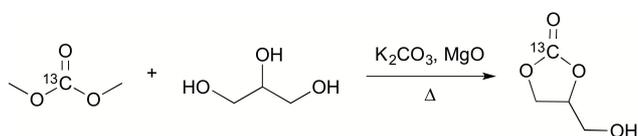
Scheme 1. Synthesis of [1-^{13}C] 1,2-glycerol carbonate.

To determine the maximum obtainable polarization of ^{13}C-GLC, as well as hydrolysis-related losses in polarization and concentration, we compared dissolutions with (n = 3) and without (n = 4) hydrolysis. ^{13}C-GLC was polarized for 3 hours and hydrolyzed with 2 equivalents of base and 10 s of heating, followed by cooling and neutralization with HCl (Figure 2a). Alternatively, the ^{13}C-GLC was dissolved in 100 mM phosphate

buffer in the non-hydrolysis experiments. A full summary of the results, including the solid-state and solution-state polarization parameters, measured T_1 values, and measures of hydrolysis completion, are listed in Table S1. Optimized conditions yielded 97.3 ± 0.5% ^{13}C $NaHCO_3$ signal as determined by peak area ratios (HP bicarbonate + CO_2 signal as a percentage of total signal), and the ^{13}C $NaHCO_3$ solution concentration was 75.1 ± 1.4 mM, corresponding to a ~30% loss from the theoretical maximum. This is presumably due to release of $^{13}CO_2$ during neutralization with HCl, which was performed in an open flask. The back-calculated polarizations with and without hydrolysis were 16.4 ± 1.3% and 18.1 ± 2.4%, respectively. The difference in polarization was not statistically significant (p > 0.30). The pH of the resulting dissolution was 7.5 ± 0.3 (n = 17), as measured with a conventional pH electrode.

We next verified that HP ^{13}C-GLC could obtain accurate pH measurements in an imaging phantom at 14 T. Three pH buffers were prepared with pH values between 6.3 and 7.4, and each buffer was added to a separate tube with about 18 U/mL of carbonic anhydrase II (CAII) to reduce the pH equilibration time.[25,30] Hydrolyzed HP ^{13}C-GLC was injected into each tube, and two 2D chemical shift imaging (CSI) pulse sequences were performed back-to-back on the same HP phantom in a vertical-bore 14 T MR imaging system maintained at 37 °C using an airflow system. The excitation pulse used in each 2D CSI was the sum of two phase-modulated Gaussian pulses, resulting in two excitation bands separated by the frequency difference between bicarbonate and CO_2 at 14 T.[31] This pulse design excited the two resonances in the same spatial location and with different degrees of excitation. The two excitation pulses used are shown in Figure 2b: one with the same degree of excitation (10° flip) for bicarbonate and CO_2, and a second involving a 2.78° flip on bicarbonate and a 25° flip on CO_2. The latter excitation pulse offers the advantage of improving the SNR of the CO_2 peak, which can be an order of magnitude lower than bicarbonate at physiological pH values. The pH was calculated from each spectrum using a modified Henderson-Hasselbalch equation, similar to that used previously:[25]

$$pH = pK_a + \log\left(\frac{S_{HCO_3^-}}{S_{CO_2}} * \frac{\sin\alpha_{CO_2}}{\sin\alpha_{HCO_3^-}}\right)$$

Here, the logarithm is taken of the bicarbonate and CO_2 spectral peak areas, corrected for the different flip angles on each resonance assuming complete magnetization exchange between excitations, and used to calculate the pH along with the pK_a, which equals 6.17 at 37 °C.[25-28] Both acquisition schemes provided spectral pH values that were within 0.1 pH unit of the pH electrode measurements (Figure 2c). The fact that the 10° and 25° CO_2 excitation schemes provide the same pH indicates that saturation of the CO_2 resonance during the 2D CSI acquisition scheme employed is not an issue due to fast bicarbonate-CO_2 exchange.[25]
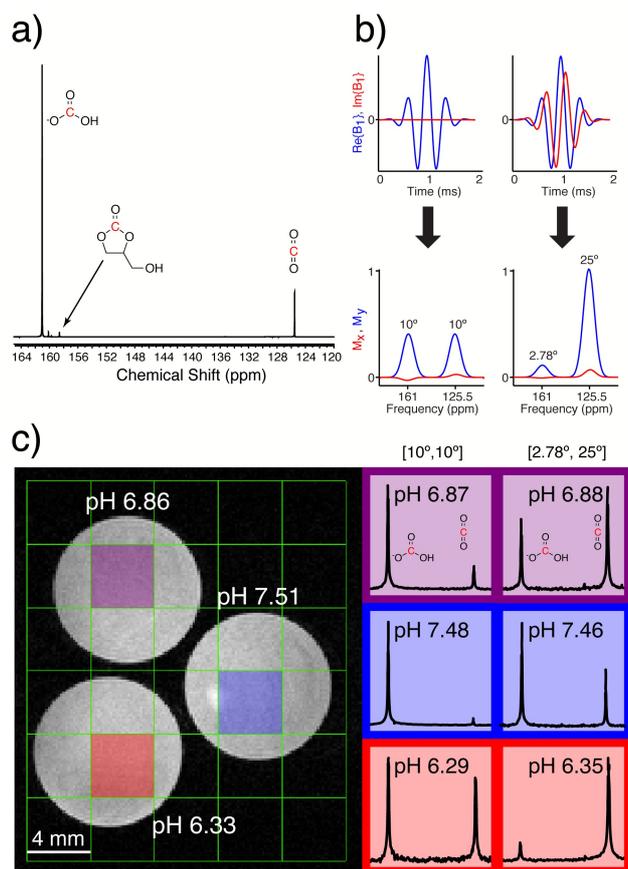
ChemComm Accepted Manuscript

Figure 2. (a) Representative ^{13}C NMR spectrum of HP ^{13}C-GLC after hydrolysis. The ^{13}C-GLC peak is referenced to 158.6 ppm. (b) Excitation pulses and simulated frequency profiles used for co-localizing HCO_3^- and CO_2 at 14 T. The degree of excitation of each resonance (bicarbonate:CO$_2$) was in the ratio of 1:1 (left) or 1:9 (right) (c) pH phantom results at 14 T: (left) T$_2$-weighted ^{1}H image, with electrode-measured pH values in white; (right) HP ^{13}C spectra and calculated pH values for each color-coded voxel in left image. Spectra were obtained using an excitation pulse from (b), as indicated above each column.

HP ^{13}C-GLC imaging of pH$_e$ was also demonstrated *in vivo* in a transgenic adenocarcinoma of the mouse prostate (TRAMP) murine model.[26] Following polarization and hydrolysis, the dissolution was injected via a tail vein catheter into an anesthetized mouse in a vertical-bore 14 T MR imaging system. A 2D CSI sequence utilizing the 2.78° bicarbonate/ 25° CO$_2$ excitation scheme was performed to obtain HP spectra from 0.2 x 0.2 x 0.8 cm^3 voxels (Figure 3). HP imaging indicated an average pH$_e$ of 7.15 ± 0.09 in the tumor (n = 13 voxels) and 7.36 ± 0.08 in adjacent benign tissue, predominantly composed of muscle and vasculature (n = 8 voxels). The pH$_e$ difference between tumor and normal tissue was about 0.2 pH units, consistent with our previous results,[26] and this difference was statistically significant (p < 1 x10^{-4}). pH$_e$ values were only calculated for voxels having bicarbonate and CO$_2$ peaks with a SNR ≥ 3. Regions of necrosis within the tumor and surrounding muscle did not satisfy these criteria. The HP bicarbonate and CO$_2$ signal from the vessel below the tumor is blurred over adjacent voxels due to the large signal magnitude and the point-spread function associated with 8 x 8 phase encoding. In separate experiments, localized dynamic ^{13}C

spectroscopy measured the apparent *in vivo* T$_1$ values of HP bicarbonate and CO$_2$ as 14.4 ± 2.4 s and 14.3 ± 3.0 s, respectively (n = 2 each). These numbers are comparable to the ~10 s T$_1$ values previously reported in mice at 9.4 T.[25] This short *in vivo* T$_1$ is an unavoidable limitation of the probe and may yield a challenge to the clinical translation of hyperpolarized ^{13}C bicarbonate based pH$_e$ imaging in general.
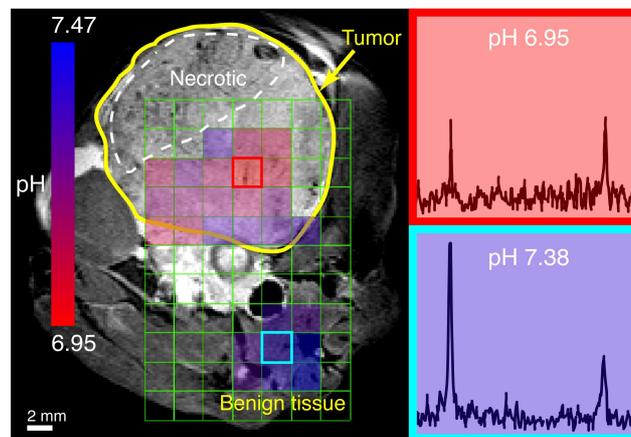

Figure 3. HP 2D CSI of hydrolyzed ^{13}C-GLC in a TRAMP mouse: (left) T$_2$-weighted ^{1}H image with overlaid pH$_e$ map calculated from HP spectra; (right) HP ^{13}C spectra for outlined voxels in left image. Prescribed in-plane resolution 0.4 cm, zero-filled to 0.2 cm; slice thickness 0.8 cm. Flip angles: 2.78° bicarbonate, 25° CO$_2$.

The carbonate precursor method reported herein may be generally applicable to the polarization of carboxylic acids, which are the most widely-used probes for ^{13}C HP.[21] Proper selection of the precursor can generate the desired HP molecule along with NaCl and other biocompatible products that do not require removal prior to injection. Previously reported strategies for HP ^{13}C-bicarbonate have demonstrated polarization values of 12-19% and concentrations of 55-100 mM while maintaining high solution-state polarization.[25-28] Our approach using ^{13}C-GLC provides comparable polarization, concentration, and spectral purity, with the additional benefit of reducing toxicity concerns, assuming the precursor is quantitatively consumed prior to injection or rapidly hydrolyzed *in vivo*. It is also important to note that a small amount of residual GLC may not be toxic since polymers of glycerol carbonate have been pursued for use in biomedical and pharmaceutical applications.[32] Although the post-dissolution step currently takes ~40 s to complete, during which there is loss of HP signal, we anticipate that simple improvements can speed up the heating and neutralization steps and thus accelerate generation of HP bicarbonate. We demonstrated that ^{13}C-GLC can measure pH *ex vivo* within 0.1 pH unit, similar to previous reports,[25,27,28] and that spatial differences in pH can be detected *in vivo*. We have demonstrated that this technique is feasible in doses ranging from 28 to 80 mg of produced ^{13}C-bicarbonate. In the only reported human clinical trial, administered doses of pyruvate ranged from approximately 250 to 1000 mg.[22] It is very likely that this technique will enable production of these amounts of probe.

Several opportunities exist for increasing the final concentration and NMR signal of the dissolution. Performing hydrolysis under pressure or within a closed apparatus may significantly reduce CO_2 losses, and process automation and use of catalysts may reduce the time necessary for full hydrolysis. Future investigations will explore the effects of these improvements, which we expect will enable use of HP ^{13}C-GLC as a clinically feasible technique for high-resolution, low-toxicity pH_e imaging.

Acknowledgements

Notes and references

1   J. L. Wike-Hooley, J. Haveman and H. S. Reinhold, *Radiotherapy and Oncology*, 1984, **2**, 343–366.
2   A. C. Williams, T. J. Collard and C. Paraskeva, *Oncogene*, 1999, **18**, 3199–3204.
3   D. Fukumura, L. Xu, Y. Chen, T. Gohongi, B. Seed and R. K. Jain, *Cancer Research*, 2001, **61**, 6020–6024.
4   K. Glunde, S. E. Guggino, M. Solaiyappan, A. P. Pathak, Y. Ichikawa and Z. M. Bhujwalla, *Neoplasia*, 2003, **5**, 533–545.
5   A. Lardner, *Journal of Leukocyte Biology*, 2001, **69**, 522–530.
6   R. A. Gatenby, E. T. Gawlinski, A. F. Gmitro, B. Kaylor and R. J. Gillies, *Cancer Research*, 2006, **66**, 5216–5223.
7   B. A. Webb, M. Chimenti, M. P. Jacobson and D. L. Barber, *Nature Publishing Group*, 2011, **11**, 671–677.
8   D. A. Rottenberg, J. Z. Ginos and K. G. Kearfott, *Annals of …*, 1985.
9   R. B. Buxton, N. M. Alpert, V. Babikian and S. Weise, *Journal of Cerebral Blood Flow and Metabolism*, 1987.
10   A. L. Vāvere, G. B. Biddlecombe, W. M. Spees, J. R. Garbow, D. Wijesinghe, O. A. Andreev, D. M. Engelman, Y. K. Reshetnyak and J. S. Lewis, *Cancer Research*, 2009, **69**, 4510–4516.
11   R. R. Flavell, C. Truillet, M. K. Regan, T. Ganguly, J. E. Blecha, J. Kurhanewicz, H. F. VanBrocklin, K. R. Keshari, C. J. Chang, M. J. Evans and D. M. Wilson, *Bioconjugate Chem.*, 2015, acs.bioconjchem.5b00584.
12   R. J. Gillies, Z. Liu and Z. Bhujwalla, *American Journal of …*, 1994.
13   M. L. Garcia-Martin, G. Herigault, C. Remy, R. Farion, P. Ballesteros, J. A. Coles, S. Cerdan and A. Ziegler, *Cancer Research*, 2001, **61**, 6524–6531.
14   P. Provent, M. Benito, B. Hiba, R. Farion, P. Lopez-Larrubia, P. Ballesteros, C. Remy, C. Segebarth, S. Cerdan, J. A. Coles and M. L. Garcia-Martin, *Cancer Research*, 2007, **67**, 7638–7645.
15   M. G. Martin and G. V. Martinez, *Magnetic resonance …*, 2006.
16   G. V. Martinez, X. Zhang and M. G. Martin, *NMR in …*, 2011.
17   D. L. Longo, W. Dastrù, G. Digilio, J. Keupp, S. Langereis, S. Lanzardo, S. Prestigio, O. Steinbach, E. Terreno, F. Uggeri and S. Aime, *Magn. Reson. Med.*, 2010, **65**, 202–211.

18   L. Q. Chen, E. A. Randtke, K. M. Jones, B. F. Moon, C. M. Howison and M. D. Pagel, *Mol Imaging Biol*, 2015.
19   J. H. Ardenkjaer-Larsen, B. Fridlund, A. Gram, G. Hansson, L. Hansson, M. H. Lerche, R. Servin, M. Thaning and K. Golman, *Proceedings of the National Academy of Sciences*, 2003, **100**, 10158–10163.
20   A. Comment and M. E. Merritt, *Biochemistry*, 2014, **53**, 7333–7357.
21   K. R. Keshari and D. M. Wilson, *Chemical Society reviews*, 2014.
22   S. J. Nelson, J. Kurhanewicz, D. B. Vigneron, P. E. Z. Larson, A. L. Harzstark, M. Ferrone, M. van Criekinge, J. W. Chang, R. Bok, I. Park, G. Reed, L. Carvajal, E. J. Small, P. Munster, V. K. Weinberg, J. H. Ardenkjaer-Larsen, A. P. Chen, R. E. Hurd, L. I. Odegardstuen, F. J. Robb, J. Tropp and J. A. Murray, *Science Translational Medicine*, 2013, **5**, 198ra108–198ra108.
23   R. R. Flavell, C. von Morze, J. E. Blecha, D. E. Korenchan, M. Van Criekinge, R. Sriram, J. W. Gordon, H.-Y. Chen, S. Subramaniam, R. A. Bok, Z. J. Wang, D. B. Vigneron, P. E. Larson, J. Kurhanewicz and D. M. Wilson, *Chemical Communications*, 2015, **51**, 14119–14122.
24   W. Jiang, L. Lumata, W. Chen, S. Zhang, Z. Kovacs, A. D. Sherry and C. Khemtong, *Sci. Rep.*, 2015, **5**, 9104.
25   F. A. Gallagher, M. I. Kettunen, S. E. Day, D.-E. Hu, J. H. Ardenkjaer-Larsen, R. I. T. Zandt, P. R. Jensen, M. Karlsson, K. Golman, M. H. Lerche and K. M. Brindle, *Nature*, 2008, **453**, 940–943.
26   D. M. Wilson, K. R. Keshari, P. E. Z. Larson, A. P. Chen, S. Hu, M. V. Criekinge, R. Bok, S. J. Nelson, J. M. Macdonald, D. B. Vigneron and J. Kurhanewicz, *Journal of Magnetic Resonance*, 2010, **205**, 141–147.
27   D. J. Scholz, M. A. Janich, U. Köllisch, R. F. Schulte, J. H. Ardenkjaer-Larsen, A. Frank, A. Haase, M. Schwaiger and M. I. Menzel, *Magn. Reson. Med.*, 2014, n/a–n/a.
28   R. K. Ghosh, S. J. Kadlecek, M. Pourfathi and R. R. Rizi, *Magn. Reson. Med.*, 2014, n/a–n/a.
29   G. Parameswaram, M. Srinivas, B. Hari Babu, P. S. Sai Prasad and N. Lingaiah, *Catal. Sci. Technol.*, 2013, **3**, 3242.
30   F. A. Gallagher, H. Sladen, M. I. Kettunen, E. M. Serrao, T. B. Rodrigues, A. Wright, A. B. Gill, S. McGuire, T. C. Booth, J. Boren, A. McIntyre, J. L. Miller, S. H. Lee, D. Honess, S. E. Day, D. E. Hu, W. J. Howat, A. L. Harris and K. M. Brindle, *Cancer Research*, 2015, **75**, 4109–4118.
31   S. L. Patt, *Journal of Magnetic Resonance (1969)*, 1992, **96**, 94–102.
32   H. Zhang and M. W. Grinstaff, *J. Am. Chem. Soc.*, 2013, **135**, 6806–6809.

ChemComm Accepted Manuscript